



Title	Suppression of in-plane tunneling anisotropic magnetoresistance effect in Co ₂ MnSi/MgO/n-GaAs and CoFe/MgO/n-GaAs junctions by inserting a MgO barrier
Author(s)	Akiho, Takafumi; Uemura, Tetsuya; Harada, Masanobu; Matsuda, Ken-ichi; Yamamoto, Masafumi
Citation	Applied Physics Letters, 98(23), 232109 https://doi.org/10.1063/1.3595311
Issue Date	2011-06-06
Doc URL	http://hdl.handle.net/2115/46768
Rights	Copyright 2011 American Institute of Physics. This article may be downloaded for personal use only. Any other use requires prior permission of the author and the American Institute of Physics. The following article appeared in Appl. Phys. Lett. 98, 232109 (2011) and may be found at https://dx.doi.org/10.1063/1.3595311
Type	article
File Information	APL98-23_232109.pdf



[Instructions for use](#)

Suppression of in-plane tunneling anisotropic magnetoresistance effect in $\text{Co}_2\text{MnSi}/\text{MgO}/\text{n-GaAs}$ and $\text{CoFe}/\text{MgO}/\text{n-GaAs}$ junctions by inserting a MgO barrier

Takafumi Akiho, Tetsuya Uemura,^{a)} Masanobu Harada, Ken-ichi Matsuda, and Masafumi Yamamoto

Division of Electronics for Informatics, Hokkaido University, Sapporo 060-0814, Japan

(Received 19 March 2011; accepted 7 May 2011; published online 9 June 2011)

The effects of MgO tunnel barriers on both junction resistance and tunneling anisotropic magnetoresistance (TAMR) characteristics of $\text{Co}_2\text{MnSi}(\text{CMS})/\text{MgO}/\text{n-GaAs}$ junctions and $\text{Co}_{50}\text{Fe}_{50}(\text{CoFe})/\text{MgO}/\text{n-GaAs}$ junctions were investigated. The resistance-area (RA) product of the CMS/MgO/n-GaAs junctions showed an exponential dependence on MgO thickness (t_{MgO}), indicating that the MgO layer acts as a tunneling barrier. The RA product of CMS/MgO/n-GaAs with $t_{\text{MgO}} < 1$ nm was smaller than that of the sample without MgO. The observed spin-valvelike magnetoresistance of CMS/n-GaAs and CoFe/n-GaAs Schottky tunnel junctions attributed to the TAMR effect did not appear in the cases of CMS/MgO/n-GaAs and CoFe/MgO/n-GaAs tunnel junctions. The lowering of the RA product and the suppression of the TAMR effect caused by inserting a thin MgO layer between CMS and n-GaAs were both possibly due to suppression of the Fermi-level pinning of GaAs and lowering of the Schottky barrier height. © 2011 American Institute of Physics. [doi:10.1063/1.3595311]

The injection of spin-polarized electrons from a ferromagnet (F) into a semiconductor (SC) is one of the most important challenges in spintronics. In particular, spin injection into GaAs or silicon by using F/SC Schottky tunnel junctions or F/insulator (I)/SC tunnel junctions has been investigated intensively.^{1–3} To achieve efficient spin injection, highly spin-polarized ferromagnetic electrodes are necessary. One cobalt-based Heusler alloy, Co_2MnSi (CMS), is a promising candidate material. We recently developed fully epitaxial magnetic tunnel junctions (MTJs) using CMS,^{4–6} and with these demonstrated high tunnel magnetoresistance (MR) ratios of up to 1135% at 4.2 K and 236% at room temperature (RT), indicating that CMS has high spin polarization. Aiming to apply CMS to a ferromagnetic electrode as an efficient spin injector into SCs, we also investigated the spin-dependent transport properties of CMS/n-GaAs Schottky tunnel junctions, and observed a tunneling anisotropic MR (TAMR) effect.⁷ Similar TAMR was also observed in Fe/GaAs/Au tunnel junctions⁸ and $\text{Co}_{50}\text{Fe}_{50}(\text{CoFe})/\text{n-GaAs}$ Schottky tunnel junctions.^{9,10} Since the TAMR effect occurs even in the case of a single F/SC junction and produces a spin-valvelike MR, it may affect the electrical detection of spin injection when F/SC heterojunctions are used. Clarifying the TAMR effect in the case of F/I/SC tunnel junctions is also important because spin injection using F/I/SC tunnel junctions was recently investigated.^{2,3} In this study, we investigated the effects of MgO tunnel barriers on the TAMR characteristics of CMS/MgO/n-GaAs and CoFe/MgO/n-GaAs tunnel junctions.

Layer structures consisting of (from the substrate side) i-GaAs (250 nm thick), n⁻-GaAs ($\text{Si} = 4 \times 10^{16} \text{ cm}^{-3}$, 300 nm), and n⁺-GaAs ($\text{Si} = 5 \times 10^{18} \text{ cm}^{-3}$, 30 nm) were grown by molecular beam epitaxy at 600 °C on GaAs (001) substrates. The samples were then capped with an arsenic pro-

TECTIVE layer and transported to a magnetron sputtering chamber. After the arsenic cap was removed by heating the samples to 300–400 °C, a MgO wedge layer with thickness ranging from 0.5 to 1.5 nm was grown by electron-beam evaporation at RT. Finally, a 5-nm-thick CMS film was grown by magnetron sputtering at RT and annealed *in situ* at 350 °C. A CoFe/MgO(0.8 nm)/n-GaAs tunnel junction was also fabricated by the same procedure. Each $10 \times 50 \mu\text{m}$ junction was fabricated using standard optical lithography and Ar ion milling techniques. The current (*I*)-voltage (*V*) characteristics and MR characteristics were measured using three-terminal geometry, as shown in the inset of Fig. 2(a). The bias voltage was defined with respect to the n-GaAs.

Figures 1(a)–1(d) show reflection high-energy electron diffraction (RHEED) patterns of the CMS layers along two different azimuths $[110]_{\text{GaAs}}$ and $[100]_{\text{GaAs}}$ for CMS/GaAs and CMS/MgO/GaAs. The streak RHEED patterns indicate that the CMS layers grew epitaxially on the GaAs or on the MgO/GaAs, although slightly spotty patterns which indicate a three-dimensional growth were observed for the CMS layer on the MgO/GaAs. Note that the RHEED patterns shown in

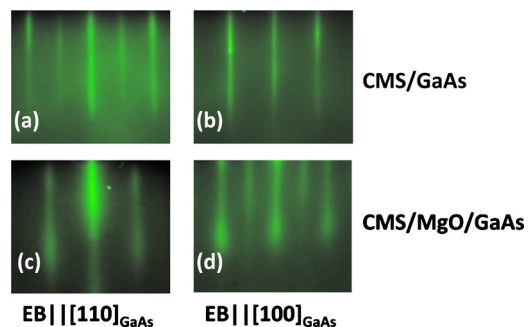


FIG. 1. (Color online) RHEED patterns along the azimuths of $[110]_{\text{GaAs}}$ and $[100]_{\text{GaAs}}$ for CMS/GaAs and CMS/MgO/GaAs. (a) CMS/GaAs with $\text{EB} \parallel [110]_{\text{GaAs}}$, (b) CMS/GaAs with $\text{EB} \parallel [100]_{\text{GaAs}}$, (c) CMS/MgO/GaAs with $\text{EB} \parallel [110]_{\text{GaAs}}$, and (d) CMS/MgO/GaAs with $\text{EB} \parallel [100]_{\text{GaAs}}$.

^{a)}Electronic mail: uemura@ist.hokudai.ac.jp.

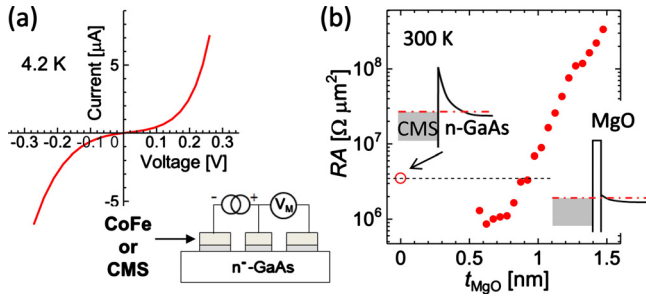


FIG. 2. (Color online) (a) Current-voltage characteristics of a $\text{Co}_2\text{MnSi(CMS)}/\text{n-GaAs}$ Schottky tunnel junction measured at 4.2 K. The inset shows a circuit configuration for three-terminal geometry. (b) RA products of CMS/MgO/n-GaAs single junctions at RT as a function of MgO thickness. The inset shows schematic band diagrams of CMS/n-GaAs junctions with and without a MgO barrier.

Figs. 1(a) and 1(d) are identical to that observed for CMS along an azimuth of $[110]_{\text{CMS}}$, and those shown in Figs. 1(b) and 1(c) are identical to that along an azimuth of $[100]_{\text{CMS}}$. Thus, the crystallographic relationship between CMS and GaAs was $\text{CMS}(001)[110] \parallel \text{GaAs}(001)[110]$ (cube-on-cube) for CMS/n-GaAs and $\text{CMS}(001)[110] \parallel \text{GaAs}(001)[100]$ for CMS/MgO/n-GaAs.

Figure 2(a) shows I - V characteristics of the CMS/n-GaAs single junction measured at 4.2 K. The I - V curve exhibited nonlinear characteristics and almost symmetric characteristics against the bias polarity due to tunneling of the electrons through a Schottky barrier formed at the CMS/n-GaAs interface. Figure 2(b) shows the resistance-area (RA) products of the CMS/MgO/n-GaAs single junctions at RT as a function of MgO thickness (t_{MgO}). The resistance was evaluated from the slope of the I - V curve at $V=0$ V measured at RT. It is noteworthy that the RA product of each sample with $t_{\text{MgO}} < 1$ nm was lower than that of the sample without a MgO layer. The RA product increased exponentially with increasing t_{MgO} , indicating that the MgO layer acted as a tunnel barrier. The $m^* \phi$ value estimated from the slope of the $\ln(\text{RA})$ versus t_{MgO} plot according to the Wenzel-Kramer-Brillouin (WKB) approximation was 0.46 eV. Here, m^* is the effective mass of a tunneling electron normalized by the bare electron mass and ϕ is the potential barrier height. This latter value (0.46 eV) was close to the value, 0.39 eV, reported for Fe/MgO/Fe MTJs (Ref. 11) with a TMR ratio of 180% at RT, and slightly larger than that, 0.32 eV, reported for $\text{Co}_2\text{Cr}_{0.6}\text{Fe}_{0.4}\text{Al}/\text{MgO}/\text{Co}_2\text{Cr}_{0.6}\text{Fe}_{0.4}\text{Al}$ MTJs with a TMR ratio of 90% at RT.¹² The tunnel resistance showing an exponential dependence on t_{MgO} and the $m^* \phi$ value being comparable to those of MTJs with relatively high TMR ratios suggest that the electrical quality of the MgO layer was high. Thus, the lowering of the RA product upon insertion of a thin MgO layer was probably due to the depinning of the Fermi-level described below rather than to a change in the layer growth mode, such as from a two-dimensional growth of the CMS layer directly grown on GaAs to a three-dimensional growth of the CMS layer grown on the MgO/GaAs, as shown in Figs. 1(c) and 1(d). It is well known that the Fermi-level of a metal/GaAs junction is pinned at the midgap of GaAs by metal-induced gap-states (MIGS) or defects. Several approaches to “depinning” the Fermi level, including insertion of a silicon interface control layer,¹³ $(\text{Gd}_{1-x}\text{Ga}_x)_2\text{O}_3/\text{Ga}_2\text{O}_3$,¹⁴ or high- k dielectrics such as Al_2O_3 and HfO_2 ,¹⁵ have been explored. The insertion of a

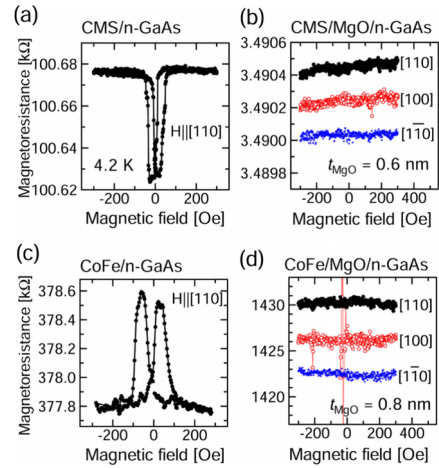


FIG. 3. (Color online) MR curves measured at 4.2 K for CMS/MgO/n-GaAs single junctions with (a) no MgO layer and (b) t_{MgO} of 0.6 nm, and those for CoFe/MgO/n-GaAs single junctions with (c) no MgO layer and (d) t_{MgO} of 0.8 nm. An in-plane magnetic field was applied along (a) $[110]$, (b) $[110]$, $[100]$, and $[1\bar{1}0]$, (c) $[110]$, and (d) $[110]$, $[100]$, and $[1\bar{1}0]$, of GaAs, respectively. The MR curves are offset for clarity in [(b) and (d)].

thin MgO barrier between the CMS and GaAs investigated in the present study also probably decreased the density of MIGS or defects formed at the CMS/GaAs interface, thereby suppressing the Fermi-level pinning and lowering the Schottky barrier height (SBH), as shown in the inset of Fig. 2(b).

Figure 3 shows MR curves measured at 4.2 K for CMS/MgO/n-GaAs single junctions with (a) no MgO layer and (b) t_{MgO} of 0.6 nm, and those for CoFe/MgO/n-GaAs single junctions with (c) no MgO layer and (d) t_{MgO} of 0.8 nm, respectively. The bias voltage was -0.15 V, and the in-plane magnetic field (H) was applied along the $[110]$ direction of GaAs for CMS/n-GaAs [Fig. 3(a)] and CoFe/n-GaAs [Fig. 3(c)], and along the $[110]$, $[100]$, and $[1\bar{1}0]$ directions for CMS/MgO/n-GaAs [Fig. 3(b)] and CoFe/MgO/n-GaAs [Fig. 3(d)]. The $[110]$ direction of GaAs corresponds to the hard-axis direction for the shape anisotropy of the junction. The curves shown in Figs. 3(b) and 3(d) are offset for clarity. The samples without a MgO barrier—i.e., the CMS/n-GaAs and CoFe/n-GaAs—showed clear MR due to the TAMR effect [Figs. 3(a) and 3(c)]. Previously, we observed uniaxial-type anisotropic tunnel resistance, or TAMR, in these samples.^{7,9,10} The angular dependence of the tunnel resistance was given by

$$R(\theta) = (R_{1\bar{1}0} - R_{110})\sin^2 \theta + R_{110}, \quad (1)$$

where θ is the angle of the magnetization (M) direction of CMS or CoFe with respect to the $[110]$ direction, and R_{110} and $R_{1\bar{1}0}$ are tunnel resistances for $M \parallel [110]$ and $M \parallel [1\bar{1}0]$, respectively. This anisotropic tunnel resistance produced a spin-valvelike MR as shown in Figs. 3(a) and 3(c). For example, in Fig. 3(a), the high-resistance state at $|H| > 100$ Oe corresponds to R_{110} , because the magnetic field is applied along the $[110]$ direction. On the other hand, the low-resistance state under a low magnetic field (i.e., $|H| < 100$ Oe) corresponds to $R_{1\bar{1}0}$ because the magnetization of CMS lies along the easy-axis direction (i.e., $[1\bar{1}0]$) under a low magnetic field. Since $R_{110} > R_{1\bar{1}0}$ for CMS/n-GaAs and vice versa for CoFe/n-GaAs at a bias voltage of -0.15 V, the

observed MR curves for the CMS (CoFe) electrode showed valleys (peaks).

On the other hand, no significant MR was observed for CMS/MgO/n-GaAs and CoFe/MgO/n-GaAs junctions, as shown in Figs. 3(b) and 3(d), although the magnetic field was swept along three different directions ($[110]$, $[100]$, and $[1\bar{1}0]$) of GaAs. These results indicate that the insertion of a MgO barrier between CMS and GaAs or between CoFe and GaAs suppressed the TAMR effect. From here, the effect of the MgO layer on the TAMR is discussed. The TAMR effect was first observed in a (Ga,Mn)As/ AlO_x /Au tunnel junction,¹⁶ and it has since been observed in several systems,^{7-10,17,18} such as a CoFe/MgO/CoFe MTJ,¹⁷ a (Co/Pt)/ AlO_x /Pt tunnel junction,¹⁸ and a Fe/GaAs/Au tunnel junction.⁸ The origin of the TAMR, however, differs depending on the system. The TAMR effect produced in a (Ga,Mn)As tunnel junction has been attributed to the anisotropic density-of-states for tunneling electrons due to spin-orbit interactions (SOIs).¹⁶ It was shown by first-principles calculations that the out-of-plane TAMR in an Fe/MgO/Fe MTJ is produced by a shift of the resonant surface states of an Fe energy band due to Rashba-SOI as the Fe magnetization rotates.¹⁹ Moser *et al.*⁸ observed uniaxial-type in-plane TAMR in a Fe/GaAs/Au tunnel junction. Our results on the TAMR effect for CoFe/n-GaAs (Ref. 9) and Co_2MnSi /n-GaAs (Ref. 7) junctions are qualitatively similar to that for Fe/GaAs/Au. Recently, Matos-Abiague and Fabian proposed a theoretical model based on the combination of Rashba and Dresselhaus SOIs for the uniaxial-type anisotropic tunnel resistance observed in Fe/GaAs/Au tunnel junctions.²⁰ The influence of the Rashba and Dresselhaus SOIs on the tunneling probability at ferromagnet/n-GaAs junctions is briefly summarized as follows. For simplicity, the Schottky barrier formed at the ferromagnet/n-GaAs interface was approximated as a single tunneling barrier with an effective barrier height of V_0 . According to the WKB approximation, the tunneling probability for electrons having Fermi energy (E_F) is given as

$$T = \exp \left[-2d \sqrt{\frac{2m}{\hbar^2} (V_0 - E_F + \mathbf{w} \cdot \mathbf{n}) + (k_x^2 + k_y^2)} \right], \quad (2)$$

where d is tunneling barrier width, \mathbf{n} is the unit vector of spin direction, and $\mathbf{k}_{\parallel} = (k_x, k_y)$ is the in-plane wave vector of a tunneling electron. $\mathbf{w} = (\alpha k_y + \beta k_x, -\alpha k_x - \beta k_y, 0)$ is the effective magnetic field induced by both Rashba SOI resulting from the structural inversion asymmetry at the interface and Dresselhaus SOI resulting from the bulk inversion asymmetry in GaAs. Here α and β are the effective Rashba and Dresselhaus parameters. By expanding Eq. (2) as a perturbative series of $\mathbf{w} \cdot \mathbf{n}$, and integrating over \mathbf{k}_{\parallel} , the anisotropic tunnel resistance given by Eq. (1) is obtained.²⁰ According to this SOI-based model, TAMR appears because of electrons tunneling through the Schottky barrier of GaAs. The lack of TAMR in the samples with a MgO barrier therefore supports the Fermi-level depinning model shown in the inset of Fig. 2(b), where the SBH is lowered by the insertion of a MgO barrier owing to the depinning of the Fermi level. In this case, the electrons tunnel only through the MgO barrier. Note

that the value of β becomes zero inside the MgO barrier, resulting in $R_{110} = R_{1\bar{1}0}$ due to a symmetric \mathbf{w} . On the other hand, out-of-plane TAMR in CoFe/MgO/CoFe-MTJs has been reported,¹⁸ and the interface resonant states are thought to cause the out-of-plane TAMR. The influence of the interface resonant states on the in-plane TAMR, however, has not yet been clarified. The change in the growth mode of the CMS/MgO layers compared to that of the CMS layer directly grown on GaAs also might affect the TAMR characteristics. Thus, further experimental and theoretical investigation is necessary to clarify the mechanism on the suppression of the TAMR effect.

In summary, we found experimentally that the RA product of CMS/MgO/n-GaAs junctions with $t_{\text{MgO}} < 1$ nm was lower than that of CMS/n-GaAs, and that the TAMR effect was suppressed in the cases of a CMS/MgO/n-GaAs junction and a CoFe/MgO/n-GaAs junction. These results are explained by the suppression of the Fermi-level pinning of GaAs and the lowering of SBH.

This work was partly supported by Grants-in-Aid for Scientific Research, and a Grant-in-Aid for Scientific Research on Priority Area "Creation and control of spin current" from the MEXT, Japan.

¹X. Lou, C. Adelman, S. A. Crooker, E. S. Garlid, J. Zhang, K. S. M. Reddy, S. D. Flexner, C. J. Palmström, and P. A. Crowell, *Nat. Phys.* **3**, 197 (2007).

²S. J. Dash, S. Sharma, R. S. Patel M. P. de Jong, and R. Jansen, *Nature (London)* **462**, 491 (2009).

³T. Sasaki, T. Oikawa, T. Suzuki, M. Shiraishi, Y. Suzuki, and K. Noguchi, *IEEE Trans. Magn.* **46**, 1436 (2010).

⁴T. Ishikawa, S. Hakamata, K.-i. Matsuda, T. Uemura, and M. Yamamoto, *J. Appl. Phys.* **103**, 07A919 (2008).

⁵T. Ishikawa, H.-x. Liu, T. Taira, K.-i. Matsuda, T. Uemura, and M. Yamamoto, *Appl. Phys. Lett.* **95**, 232512 (2009).

⁶M. Yamamoto, T. Ishikawa, T. Taira, G.-f. Li, K.-i. Matsuda, and T. Uemura, *J. Phys.: Condens. Matter* **22**, 164212 (2010).

⁷T. Uemura, M. Harada, K.-i. Matsuda, and M. Yamamoto, *Appl. Phys. Lett.* **96**, 252106 (2010).

⁸J. Moser, A. Matos-Abiague, D. Schuh, W. Wegscheider, J. Fabian, and D. Weiss, *Phys. Rev. Lett.* **99**, 056601 (2007).

⁹T. Uemura, Y. Imai, M. Harada, K.-i. Matsuda, and M. Yamamoto, *Appl. Phys. Lett.* **94**, 182502 (2009).

¹⁰T. Uemura, M. Harada, T. Akiho, K.-i. Matsuda, and M. Yamamoto, *Appl. Phys. Lett.* **98**, 102503 (2011).

¹¹S. Yuasa, T. Nagahama, A. Fukushima, Y. Suzuki, and K. Ando, *Nature Mater.* **3**, 868 (2004).

¹²T. Marukame, T. Ishikawa, W. Sekine, K.-i. Matsuda, T. Uemura, and M. Yamamoto, *IEEE Trans. Magn.* **42**, 2652 (2006).

¹³H. Hasegawa and M. Akazawa, *Appl. Surf. Sci.* **255**, 628 (2008).

¹⁴M. Passlack, M. Hong, and J. P. Mannaerts, *Appl. Phys. Lett.* **68**, 1099 (1996).

¹⁵P. D. Ye, G. D. Wilk, B. Yang, S. N. G. Chu, K. K. Ng, and J. Bude, *Solid-State Electron.* **49**, 790 (2005).

¹⁶C. Gould, C. Rüster, T. Jungwirth, E. Girgis, G. M. Schott, R. Giraud, K. Brunner, G. Schmidt, and L. W. Molenkamp, *Phys. Rev. Lett.* **93**, 117203 (2004).

¹⁷L. Gao, X. Jiang, S. Yang, J. D. Burton, E. Y. Tsymal, and S. S. P. Parkin, *Phys. Rev. Lett.* **99**, 226602 (2007).

¹⁸B. G. Park, J. Wunderlich, D. A. Williams, S. J. Joo, K. Y. Jung, K. H. Shin, K. Olejnik, A. B. Shick, and T. Jungwirth, *Phys. Rev. Lett.* **100**, 087204 (2008).

¹⁹M. N. Khan, J. Henk, and P. Bruno, *J. Phys.: Condens. Matter* **20**, 155208 (2008).

²⁰A. Matos-Abiague and J. Fabian, *Phys. Rev. B* **79**, 155303 (2009).